


RESEARCH ARTICLE

Open Access



Differences in the photosynthetic and physiological responses of *Leymus chinensis* to different levels of grazing intensity

Min Liu^{1,2}, Jirui Gong^{1*} , Bo Yang¹, Yong Ding³, Zihe Zhang¹, Biao Wang¹, Chenchen Zhu¹ and Xiangyang Hou^{3*}

Abstract

Background: Grazing is an important land use in northern China. In general, different grazing intensities had a different impact on the morphological and physiological traits of plants, and especially their photosynthetic capacity. We investigated the responses of *Leymus chinensis* to light, medium, and heavy grazing intensities in comparison with a grazing exclusion control.

Results: With light grazing, *L. chinensis* showed decreased photosynthetic capacity. The low chlorophyll and carotenoid contents constrained light energy transformation and dissipation, and Rubisco activity was also low, restricting the carboxylation efficiency. In addition, the damaged photosynthetic apparatus accumulated reactive oxygen species (ROS). With medium grazing, more energy was used for thermal dissipation, with high carotene content and high non-photochemical quenching, whereas photosynthetic electron transport was lowest. Significantly decreased photosynthesis decreased leaf C contents. Plants decreased the risk caused by ROS through increased energy dissipation. With high grazing intensity, plants changed their strategy to improve survival through photosynthetic compensation. More energy was allocated to photosynthetic electron transport. Though heavy grazing damaged the chloroplast ultrastructure, adjustment of internal mechanisms increased compensatory photosynthesis, and an increased tiller number facilitated regrowth after grazing.

Conclusions: Overall, the plants adopted different strategies by adjusting their metabolism and growth in response to their changing environment.

Keywords: Grazing intensity, Photosynthetic capacity, Chlorophyll fluorescence, Chloroplast structure, Reactive oxygen species

Background

Grazing is the most common and important land use in Inner Mongolia that affects grassland productivity and vegetation dynamics [67, 83]. In recent years, more and more grasslands have been severely damaged by long-term overgrazing, resulting in widespread grassland degradation [43, 84]. The over-grazing decreases vegetation cover and damages the soil, leading to

desertification and continuously decreasing grassland productivity, thereby damaging the structure and functions of the grassland ecosystem [6]. The dominant grassland species contribute most to the ecosystem's productivity and therefore play an important role in conferring resistance to disturbance and maintenance of stability. Therefore, it's essential that we improve our understanding of how the dominant species respond to the grazing disturbance.

Livestock grazing directly affects plant morphology. For example, it reduces plant height, decreases the length of shoot internodes, and decreases leaf area [76, 88]. Because taller plants with more leaves are more attractive to herbivores, the dwarf characteristics that result from grazing may help the plants to escape herbivores [77]. At the same time, grazed plants increase their tiller production to

* Correspondence: jrgong@bnu.edu.cn; houxly16@126.com

¹Beijing Key Laboratory of Traditional Chinese Medicine Protection and Utilization, Key Laboratory of Surface Processes and Resource Ecology, College of Resources Science and Technology, Faculty of Geographical Science, Beijing Normal University, No. 19 Xijiekouwai Street, Beijing 100875, China

³Grassland Research Institute of Chinese Academic of Agricultural Science, Hohhot 010021, Inner Mongolia, China

Full list of author information is available at the end of the article



promote rapid regrowth [87]. On the other hand, grazing stress also affected the physiological responses of plants, such as compensatory growth and changes in photosynthetic capacity [12, 49, 63].

Herbivory was formerly thought to be detrimental to plant fitness because of its metabolic effects, and particularly down-regulation of photosynthesis [26]. However, the primary response to removal of tissues by herbivory is regrowth through the reconstruction of damaged tissues and organs, which is achieved by increased CO₂ assimilation capacity. The plant responds by increasing the chlorophyll content, activity of photosynthetic enzymes, and electron transport capacity, which together improves the physiological functioning of the photosynthetic apparatus. These changes may be sufficient to compensate for the loss of photosynthetically active leaves [30, 34]. Furthermore, grazing removes old and dead plant tissues and alters the plant's mass allocation so that plants can produce more new leaves to restore their photosynthetic capacity [87, 88].

As these responses show, plants that face different grazing stress may exhibit different responses and different protection strategies. Because damage to plants increases with increasing grazing intensity, plant photosynthetic properties are also likely to change. However, we still don't fully understand the physiological changes that occur under different grazing intensities.

In general, the absorption and utilization of solar energy by plants changes in response to grazing. Plants have more light available to them after grazing due to the decreased shading, but on the other hand, the reduced leaf area may limit their ability to acquire sufficient light [70]. Increased illumination may also cause photoinhibition and decreased photosynthetic efficiency if the input of photons exceeds the plant's photosynthetic capacity [28, 46, 63]. When the excess energy cannot be safely dissipated, this leads to the accumulation of reactive oxygen species (ROS) [75, 85, 89]. The ROS suppress the synthesis of PSII proteins in the chloroplasts, increase lipid peroxidation, and damage the photosynthetic apparatus [13, 71].

CO₂ assimilation by the chloroplasts consumes energy and depends on Rubisco (ribulose 1,5-bisphosphate carboxylase) [46]. Thus, any stress that adversely affects Rubisco activity or regeneration will reduce photosynthesis. Grazing and other environmental stresses can also accelerate the degradation of chloroplasts, resulting in swollen or ruptured chloroplasts in the damaged leaves [20, 66]. Overall, the available evidence suggests that the plant's photosynthetic capacity is affected by the structural and the physiological responses to grazing [29, 68, 81]. But little information is available on the structural changes of chloroplasts and the associated regulatory mechanisms under grazing.

Plants develop many strategies to scavenge ROS and protect their photosynthetic apparatus against stress-induced damage. For example, the presence of large quantities of xanthophyll-cycle components in leaves can consume excess energy and provide protection against excessive light energy, thereby reducing the production of ROS [53]. At the same time, the plant's system of antioxidant enzymes, which include superoxide dismutase (SOD), catalase (CAT), ascorbate peroxidase, glutathione peroxidase, and peroxidase (POD), plays a crucial role in scavenging ROS [4, 11]. In addition, up-regulation of proline production can mitigate the reduction in peroxidase and catalase activity that sometimes occurs under stress [33]. Proline can decrease ROS levels and delay or prevent cell death [10]. In addition, proline accumulation makes the cell osmotic potential more negative, thereby increasing resistance to the water stress that results from grazing damage [27]. Although many studies have illustrated the roles of these antioxidant enzymes, the relationship between the stress and enzyme activity is not clear. The specific strategies that plants adopt to cope with stress, and the relationship of these strategies to the plant's grazing tolerance, are still mostly unknown and need to be discovered.

Grasslands cover almost 42% of the earth's surface and account for about 34% of the global terrestrial organic carbon storage, which makes them a widespread and important vegetation type [68]. In China, grassland covers more 40% of the total land area [37]. As the main temperate grassland of northern China, Inner Mongolia's grasslands play a crucial role in environmental protection and livestock production [86]. However, the grasslands are fragile and sensitive to human disturbance, and especially to irrational utilization and unsustainable development [42, 82]. To provide some of the missing knowledge of grazing effect on grassland, we designed the present study to examine the effects of four different grazing intensities (a control with grazing exclusion, and light, medium, and heavy grazing) on the photosynthetic capacity of *Leymus chinensis*, a key species in northern China's grassland ecosystems. *L. chinensis* is the widely distributed grass in Inner Mongolia's grasslands. It is a perennial C3 grass, with the long and strong rhizomes. *L. chinensis* shows a vigorous vegetative propagation in the grassland [45]. To do so, we measured gas exchange, chlorophyll fluorescence, photosynthetic enzyme activity, pigment contents, and the ultrastructure of the chloroplasts. We also measured the peroxidation of membrane lipids and the plant's antioxidant system. Our specific objectives were (i) to clarify the photosynthetic response and adaptation mechanisms of *L. chinensis* at different grazing intensities; (ii) to examine the relationship between the structural changes of chloroplasts and physiological regulation of photosynthesis under the different

grazing intensities; and (iii) to identify the equilibrium between the generation and elimination of ROS.

Results

Plant morphological traits and soil traits

The morphological characteristics of *L. chinensis* differed significantly among the four grazing plots (Table 1, $P < 0.05$). SLA was highest in the LG plots and lowest in the MG plots. The tiller number increased with increasing grazing intensity, and the difference was significant in the HG plots, whereas the mean internode length decreased gradually, and the difference was significant for all grazing intensities. Plant biomass and height decreased with increasing grazing intensity, and the differences became significant in the HG and MG plots, respectively. Especially in the HG plots, the biomass and height reduced by half. Leaf osmotic potential decreased (became more negative, indicating greater water stress) with increasing grazing intensity, and the difference was significant in the MG and HG plots.

The characteristics of soil were significantly different among the four grazing plots (Table 1, $P < 0.05$). Compare with soil in the control plots, soil in the LG and MG plots was moister, and driest in the HG plots. Similar with the soil water content, the soil nitrogen and carbon contents were higher in the LG and MG plots than those in the control plots, and lowest in the HG plots. In contrast, the soil available phosphorus mainly decreased as the grazing intensity increased.

The leaf C, N, and P contents

The leaf C, N and P contents showed different trends with increasing grazing intensity (Fig. 1). The leaf C content was significantly lower in the MG plots than in the other plots, which did not differ significantly from each other. Leaf N content was significantly higher in the HG plots, but there was no significant difference among the

other three plots. In contrast, the P content was significantly higher than in the control in the LG plots, and significantly lower than in the control and in the MG and HG plots.

The photosynthetic pigment contents and Rubisco activity

Figure 2 shows the leaf contents of the photosynthetic pigments. The contents differed significantly among the grazing intensities ($P < 0.05$). The Chl *a*, Car, and Chl *a* + *b* contents were significantly lower than in the control in the LG plots, but the LG values were significantly lower than in the MG and HG plots. In contrast, the Chl *b* content and the Chl *a/b* ratio did not differ significantly among the grazing intensities. The Rubisco activity increased with increasing grazing intensity, but was significantly lower than in the control and in the LG plots and significantly higher in the HG plots.

Leaf gas-exchange and chlorophyll fluorescence parameters

Table 2 summarized the leaf gas-exchange and response curves characteristics. These differed significantly among the grazing intensities ($P < 0.05$). In the control plots, *L. chinensis* had significantly higher P_n and WUE than in the grazed plots, but significantly lower *E*. In the LG plots, LSP, and AQY were significantly higher than in the other plots and LCP was significantly lower. In the MG plots, P_n and WUE were significantly lower than those in the control. In the HG plots, *E* was significantly higher than in the other grazed plots. R_d was significantly lower in the LG and HG plots than in the control and MG plots, but did not differ significantly between LG and HG or between the control and MG. Table 2 also summarizes the data from the leaf CO₂-response curves. All four parameters differed significantly among the grazing intensities ($P < 0.05$). J_{max} , V_{cmax} and V_{TPU}

Table 1 The morphological traits of *L. chinensis* and the soil characteristics in the plots with different grazing intensities

Parameter	Control	LG	MG	HG
Specific leaf area (cm ² g ⁻¹)	116.1 ± 2.6b	143.4 ± 3.7a	100.6 ± 4.1c	118.8 ± 6.9b
Tiller number	3.4 ± 0.5b	4.0 ± 0.4ab	4.2 ± 0.4ab	5.3 ± 0.3a
Mean internode length (cm)	6.1 ± 0.1a	5.4 ± 0.3b	2.4 ± 0.2c	2.4 ± 0.2c
Plant height (cm)	26.3 ± 0.8a	24.6 ± 1.1a	20.4 ± 0.7a	13.2 ± 1.6b
Plant biomass (g m ⁻²)	35.1 ± 1.7a	31.3 ± 2.0ab	27.6 ± 2.4b	15.2 ± 1.0c
Leaf osmotic potential (MPa)	-1.6 ± 0.04a	-1.9 ± 0.019ab	-3.0 ± 0.04b	-2.8 ± 0.92b
Soil water content (%)	5.77 ± 0.93c	7.60 ± 0.08b	8.95 ± 0.11a	4.53 ± 0.08d
Soil nitrogen content (%)	0.15 ± 0.003b	0.17 ± 0.003a	0.16 ± 0.001a	0.14 ± 0.003c
Soil carbon content (%)	1.47 ± 0.018c	1.64 ± 0.005a	1.54 ± 0.015b	1.37 ± 0.006d
Soil available phosphorus (%)	405.6 ± 0.66a	389.0 ± 6.22b	390.2 ± 3.29b	358.8 ± 1.57c

Values are means ± SE. Values in a column labeled with different letters differ significantly (ANOVA followed by LSD test, $P < 0.05$)
Control no grazing, LG light grazing, MG medium grazing, HG heavy grazing

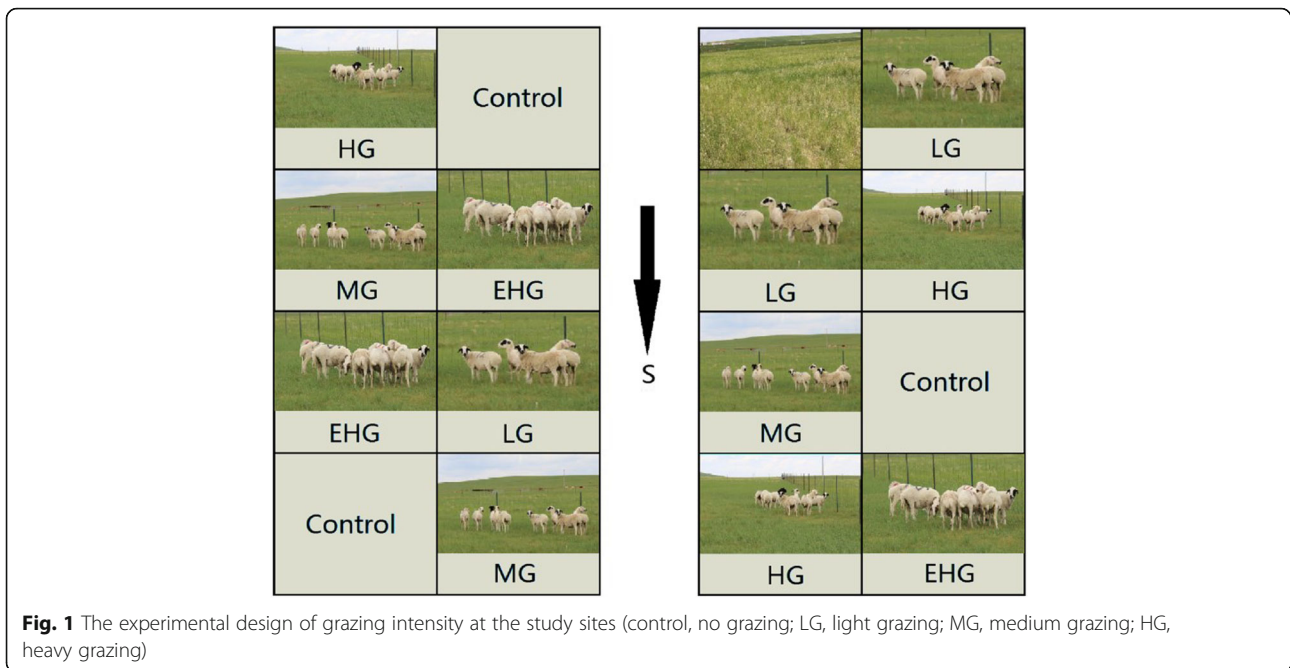


Fig. 1 The experimental design of grazing intensity at the study sites (control, no grazing; LG, light grazing; MG, medium grazing; HG, heavy grazing)

were significantly higher in the LG plots than in the other plots, and significantly lower in the control plots. In contrast, the J_{max} / V_{cmax} ratios were lower in the MG plots and significantly higher in the HG plots.

Table 3 summarizes the leaf chlorophyll fluorescence parameters, which differed significantly among the grazing intensities ($P < 0.05$). There was no significant difference in F_v/F_m , qP , and NPQ among the plots. In the control plots, the values of F_v'/F_m' were significantly higher than those in the other plots. In the LG plots, F_m and F_v'/F_m' were significantly lower than in the control. In the MG plots, F_0 , F_m , F_v'/F_m' , and Φ_{PSII}

were significantly lower than in the other plots. Compared with the MG plots, more energy was used for photosynthetic electron transport in the HG plots and less was used in the MG plots. Thermal dissipation was higher and excess energy was lower than in the control in all of the grazed plots (Fig. 3).

In the control plots, the chloroplasts were intact, with an orderly arrangement of grana and of the stroma lamellae and well-developed thylakoid membranes (Fig. 4a). In the LG plots, starch grains were occasionally observed in the chloroplasts (Fig. 4b). There was no obvious difference of chloroplast

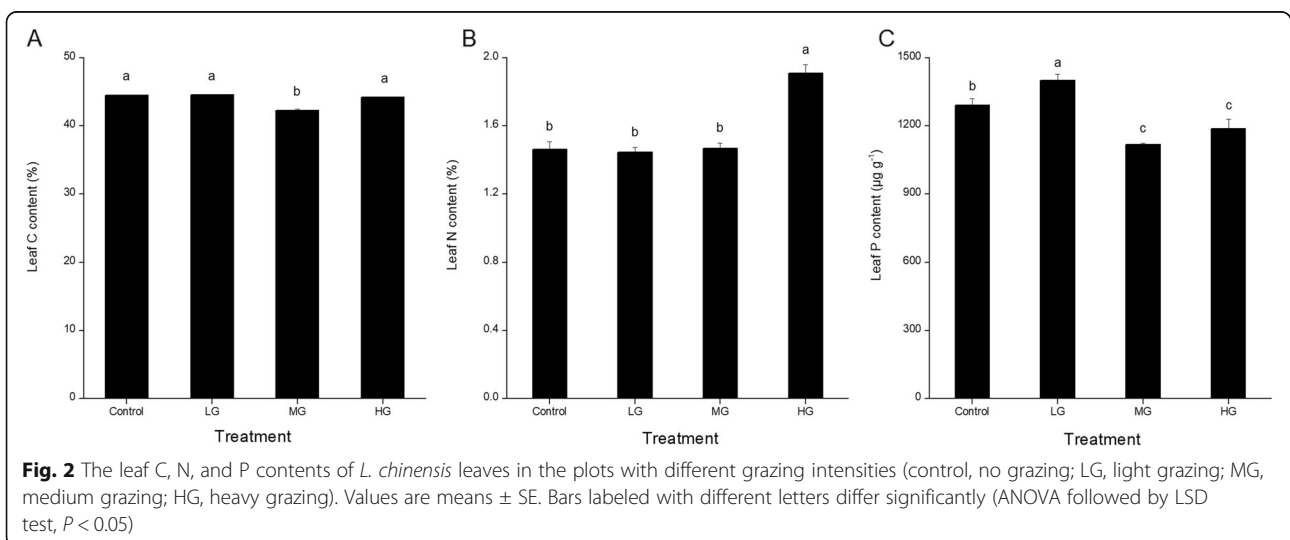


Fig. 2 The leaf C, N, and P contents of *L. chinensis* leaves in the plots with different grazing intensities (control, no grazing; LG, light grazing; MG, medium grazing; HG, heavy grazing). Values are means \pm SE. Bars labeled with different letters differ significantly (ANOVA followed by LSD test, $P < 0.05$)

Table 2 The gas-exchange characteristics and the light and CO₂-response curve parameters of *L. chinensis* in the plots with different grazing intensities

	Control	LG	MG	HG
P_n ($\mu\text{mol m}^{-2} \text{s}^{-1}$)	8.46 ± 0.99a	1.64 ± 0.14bc	0.75 ± 0.34c	3.24 ± 0.76b
T_r ($\text{mmol m}^{-2} \text{s}^{-1}$)	0.67 ± 0.09d	1.98 ± 0.24b	1.46 ± 0.12c	2.73 ± 0.01a
WUE ($\mu\text{mol mmol}^{-1}$)	13.65 ± 3.77a	0.83 ± 0.02b	0.51 ± 0.23b	1.18 ± 0.28b
LSP ($\mu\text{mol}\cdot\text{m}^{-2} \text{s}^{-1}$)	492 ± 1.2b	712 ± 4.5a	501 ± 6.4b	542 ± 2.8b
LCP ($\mu\text{mol}\cdot\text{m}^{-2} \text{s}^{-1}$)	68 ± 3.2a	28 ± 1.2b	54 ± 4.1a	32 ± 2.0b
R_d ($\mu\text{mol}\cdot\text{m}^{-2} \text{s}^{-1}$)	2.50 ± 0.18a	1.37 ± 1.24b	2.84 ± 0.21a	1.22 ± 1.28b
AQY ($\mu\text{mol CO}_2 \mu\text{mol}^{-1}$)	0.039 ± 0.01b	0.049 ± 0.02a	0.037 ± 0.01b	0.039 ± 0.01b
J_{max} ($\mu\text{mol}\cdot\text{m}^{-2} \text{s}^{-1}$)	22.42 ± 1.32d	48.10 ± 2.40a	27.49 ± 2.34c	31.19 ± 1.36b
V_{cmax} ($\mu\text{mol}\cdot\text{m}^{-2} \text{s}^{-1}$)	21.89 ± 0.24c	44.30 ± 5.42a	27.34 ± 1.86b	28.29 ± 3.42b
V_{TPU} ($\mu\text{mol}\cdot\text{m}^{-2} \text{s}^{-1}$)	5.22 ± 0.23c	10.27 ± 0.89a	6.82 ± 0.58b	6.25 ± 0.56b
$J_{\text{max}}/V_{\text{cmax}}$	1.024 ± 0.02b	1.085 ± 0.03b	1.005 ± 0.01c	1.102 ± 0.03a

Values are means ± SE (n = 3). Values of a parameter labeled with different letters differ significantly between light intensities (ANOVA followed by LSD test, $P < 0.05$)

Control no grazing, LG light grazing, MG medium grazing, HG heavy grazing, P_n net photosynthetic rate, T_r transpiration rate, WUE water-use efficiency, LSP light saturation point, LCP light compensation point, R_d dark respiration rate, AQY apparent quantum yield, J_{max} maximum electron transport rate, V_{cmax} maximum carboxylation efficiency, V_{TPU} triose phosphate utilization rate

ultrastructure among the grazing intensity except in the HG plots, where the chloroplasts were swollen and had irregular grana (Fig. 4d). In addition, the degraded osmiophilic granule became common in the chloroplasts in the HG plots.

Table 3 The chlorophyll fluorescence parameters of *L. chinensis* in the plots with different grazing intensities

	Control	LG	MG	HG
F_o	133.9 ± 6.53c	184.3 ± 5.58a	123.8 ± 6.70c	155.8 ± 2.51b
F_m	646.5 ± 13.0a	624.9 ± 46.1ab	502.2 ± 30.0c	599.3 ± 23.5b
F_v/F_m	0.79 ± 0.005a	0.76 ± 0.006a	0.78 ± 0.001a	0.77 ± 0.005a
F_v'/F_m'	0.501 ± 0.021a	0.424 ± 0.001b	0.377 ± 0.005c	0.446 ± 0.013b
q_p	0.509 ± 0.056a	0.583 ± 0.027a	0.503 ± 0.036a	0.595 ± 0.007a
NPQ	1.305 ± 0.230a	1.328 ± 0.557a	1.545 ± 0.444a	1.289 ± 0.252a
ETR	166.8 ± 16.8ab	130.0 ± 6.24b	150.0 ± 13.0ab	174.4 ± 6.77a
Φ_{PSII}	0.254 ± 0.025a	0.247 ± 0.012a	0.190 ± 0.016b	0.266 ± 0.010a

Values are means ± SE (n = 3). Values of a parameter labeled with different letters differ significantly between light intensities (ANOVA followed by LSD test, $P < 0.05$)

Control no grazing, LG light grazing, MG medium grazing, HG heavy grazing, F_o minimum fluorescence, F_m maximum fluorescence, F_v/F_m the maximum quantum efficiency of PSII, F_v'/F_m' energy harvesting efficiency of PSII, q_p photochemical quenching coefficient, NPQ non-photochemical quenching coefficient, ETR electron transport rate, Φ_{PSII} effective quantum yield of PSII

Lipid peroxidation and antioxidant systems

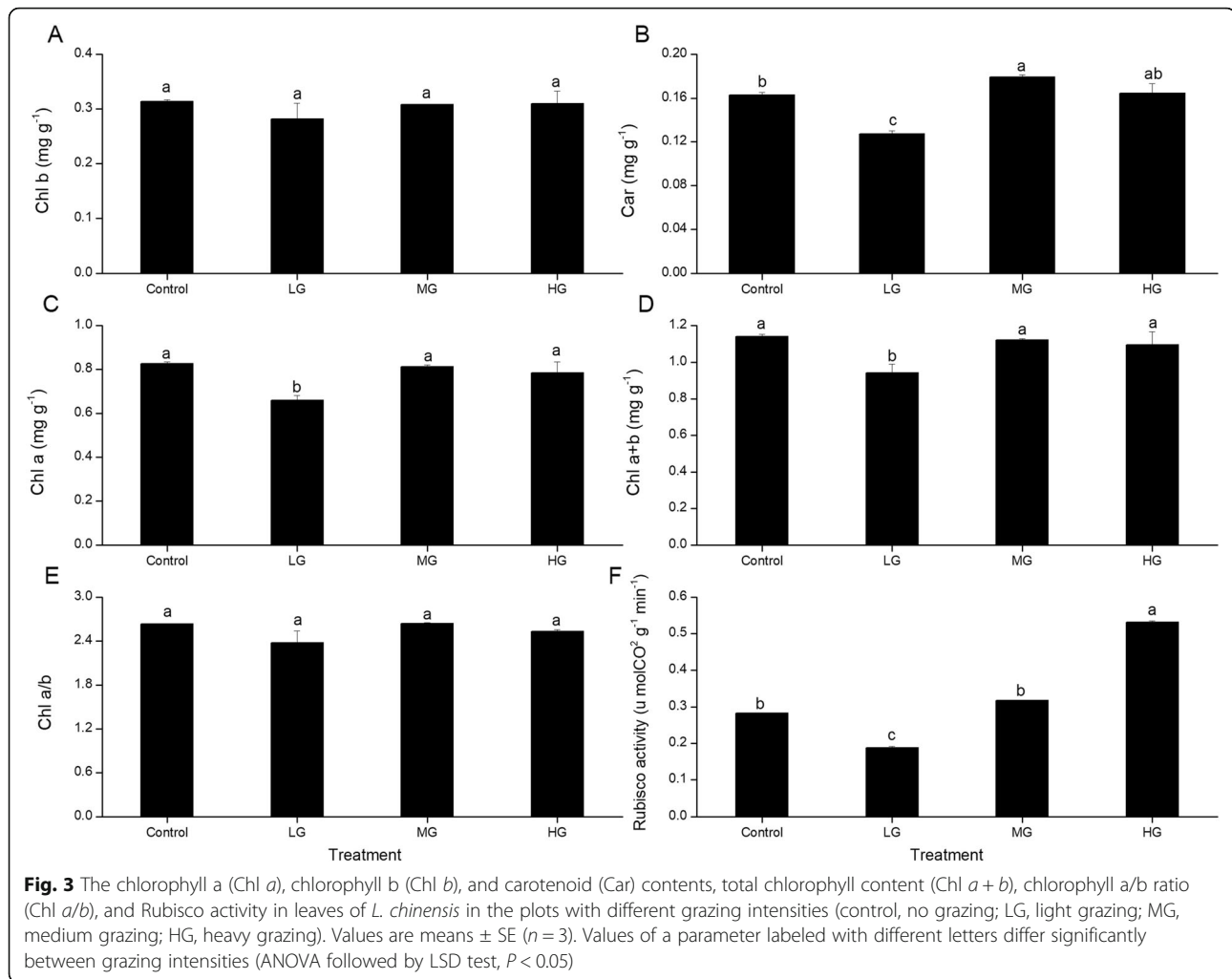
The degree of membrane lipid peroxidation differed significantly among the grazing intensities (Fig. 5, $P < 0.05$). The MDA contents of the leaves were significantly higher in the grazed plots than in the control, but did not differ significantly among the grazed plots.

The leaves had significantly higher proline contents in the MG plots than in the other plots, which did not differ significantly (Fig. 6a). SOD activity was significantly lower in the HG plots than in the other plots, which did not differ significantly. POD activity was significantly lower in the LG plots than in the other plots, and significantly higher in the HG plots. CAT activity was significantly higher in the MG plots than in the control, but did not differ significantly among the other plots.

Discussion

Morphological changes in response to increasing grazing intensity

Morphological changes of plants are a primary response to environmental stresses. As the main organ consumed by herbivores, the leaves of *L. chinensis* were significantly influenced by herbivory. SLA is an important indicator of leaf function, as it represents the plant's ability to acquire and utilize resources, as well as the plant's

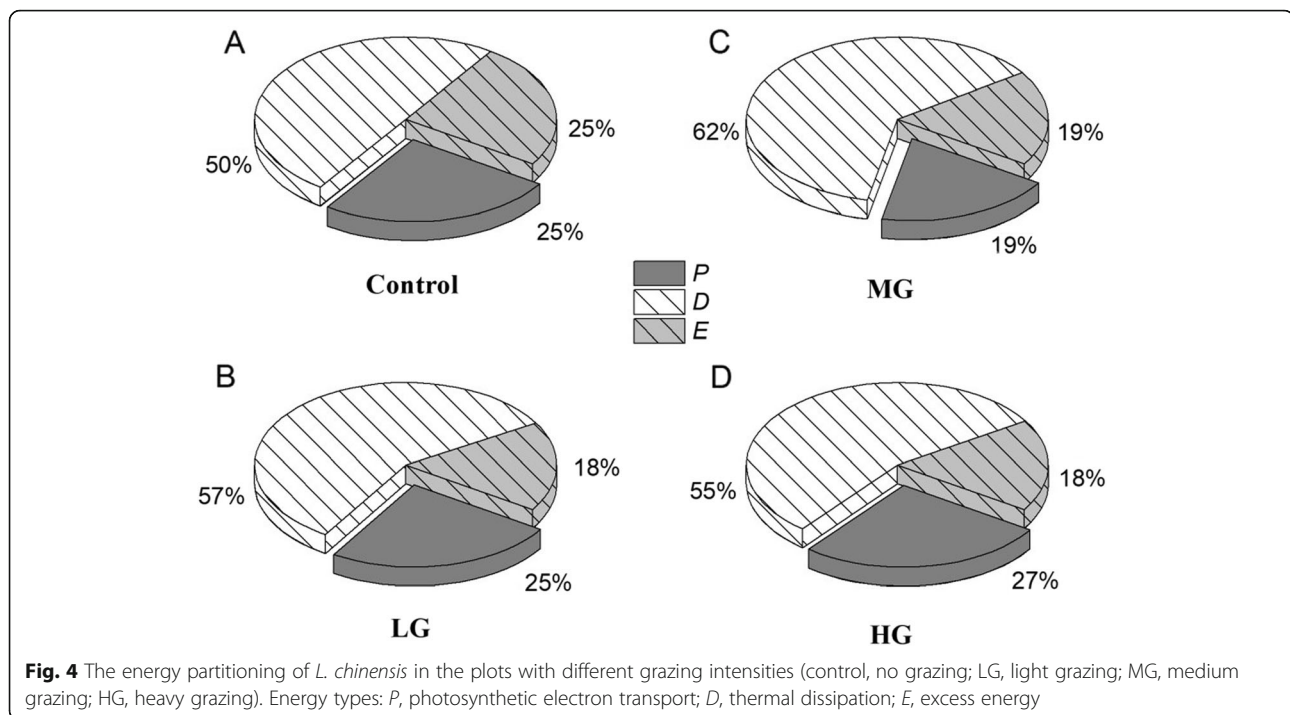


allocation of resources among different uses [36]. In the LG plots, *L. chinensis* had the highest SLA, which means that *L. chinensis* can grow new leaves fastest after light herbivory and that its response to the uneven distribution of light resources became more flexible [25, 60]. Plants with high SLA can respond more easily to a resource-rich environment, such as the increased C, N contents in the soil or the availability of light after grazing. However, high SLA also indicates thinner cell walls, which makes the leaves more vulnerable to damage by herbivores [78]. In contrast, the low SLA in the MG plots suggested that the leaves became thicker than those in the control and probably lasted longer. Meanwhile, leaves accumulated more assimilate per unit area, which would offer some protection against herbivores [36, 44]. At the same time, the steadily decreasing plant height and internode length with increasing grazing intensity produced plants with more of a dwarf phenotype, which may represent a grazing avoidance strategy that protects the plants. On the other hand, the increase in tiller number with increasing grazing intensity would promote regrowth of the plants, and could also represent a grazing

tolerance mechanism [65]. At the heavy grazing intensity, roots of *L. chinensis* absorbed more nutrients rapidly from the soil to grow complementally, which also reduced the soil nutrient in the heavy grazing plots [76]. With increasing grazing intensity, plant biomass gradually decreases [62]. Once the pressure from grazing was removed, the proportion of *L. chinensis* in the vegetation cover would increase again. However, while grazing continues, dwarfing of the grazed plants can directly decrease grassland productivity [88]. Different grazing intensities resulted in the different morphological responses. However, we did not find the obvious morphological compensatory growth.

Photosynthetic responses and adaptation to increasing grazing intensity

In addition to the abovementioned morphological changes, *L. chinensis* will adapt its physiology in response to the disturbance and to the resulting changes in resource availability [40, 70]. Grazing, herbivores will change light availability and thereby affect acquisition of this resource by plants, thereby affecting their physiological characteristics. Plant



photosynthesis is a particularly important indicator of physiological sensitivity to environmental stress because this process provides the energy that plants need to survive and adapt [7]. In the present study, the photosynthetic rates of *L. chinensis* in the LG and MG plots were significantly lower than in the control, but increased in the HG plots. This suggests that the plants performed compensatory photosynthesis in response to the severe loss of leaves in the HG plots [15, 42]. In the LG plots, *L. chinensis* had a high LSP and low LCP, thereby allowing the plants to maximize their utilization of the available light energy. On the other hand, the plants had lower quantities of the photosynthetic pigments. The changes in the amounts and composition of the photosynthetic pigments reflect underlying functional modifications of the photosynthetic apparatus, thereby causing photosynthetic performance to change in a coordinated manner [17, 21]. Photosynthetic pigments are sensitive to environmental changes, making them potentially suitable as biomarkers [48]. Our results suggest that light grazing may inhibit chlorophyll synthesis or increase the activity of chlorophyll-degrading enzymes [61]. Through the chlorophyll cycle, Chl *b* can be converted into Chl *a*. This interconversion gives plants the ability to optimally adapt to changing light conditions [61]. There was no significant difference in Chl *a/b* among grazing plots. As Chl *b* is only present in the light-harvesting phase and not the light energy transformation phase, the lower Chl *a/b* suggests that they invested more in the absorption

of light energy. If the photosystems had significantly larger antenna sizes (a significantly lower Chl *a/b* ratio), this could represent more optimal use of the low light intensity that would exist when there was little reduction of the vegetation cover [18, 73].

On the other hand, more absorbed light energy cannot always be fully used to support photosynthesis, and the excess energy must be dissipated. The increased thermal energy dissipation in all grazed plots was accompanied by increased F_o , which may indicate the degradation of the D1 protein in PSII or disruption of the energy transfer into the reaction center [31]. Under stress, F_o would increase but F_v/F_m would decrease [51]. Two factors may lead to this situation: a reduction of the plastoquinone electron receptors or incomplete oxidation, which delays the electron transfer chain in PSII; the damage to the light-harvesting phyllochlorin [5]. Therefore, plants had lower ETR and higher ROS accumulation (as measured by the MDA content) in the LG plots. The increase of F_o , together with the decreased ETR and F_v/F_m in the LG plots indicated damage to the photosynthetic apparatus, which would also explain the decreased Rubisco activity [41]. In addition, there is often a correlation between F_o and the Chl contents in the plants: F_o increases with decreasing Chl content. We observed starch grains in the chloroplasts in the LG plots. This may be due to damage to the photosynthetic apparatus. The photosynthesis-synthesized sugars cannot be exported or

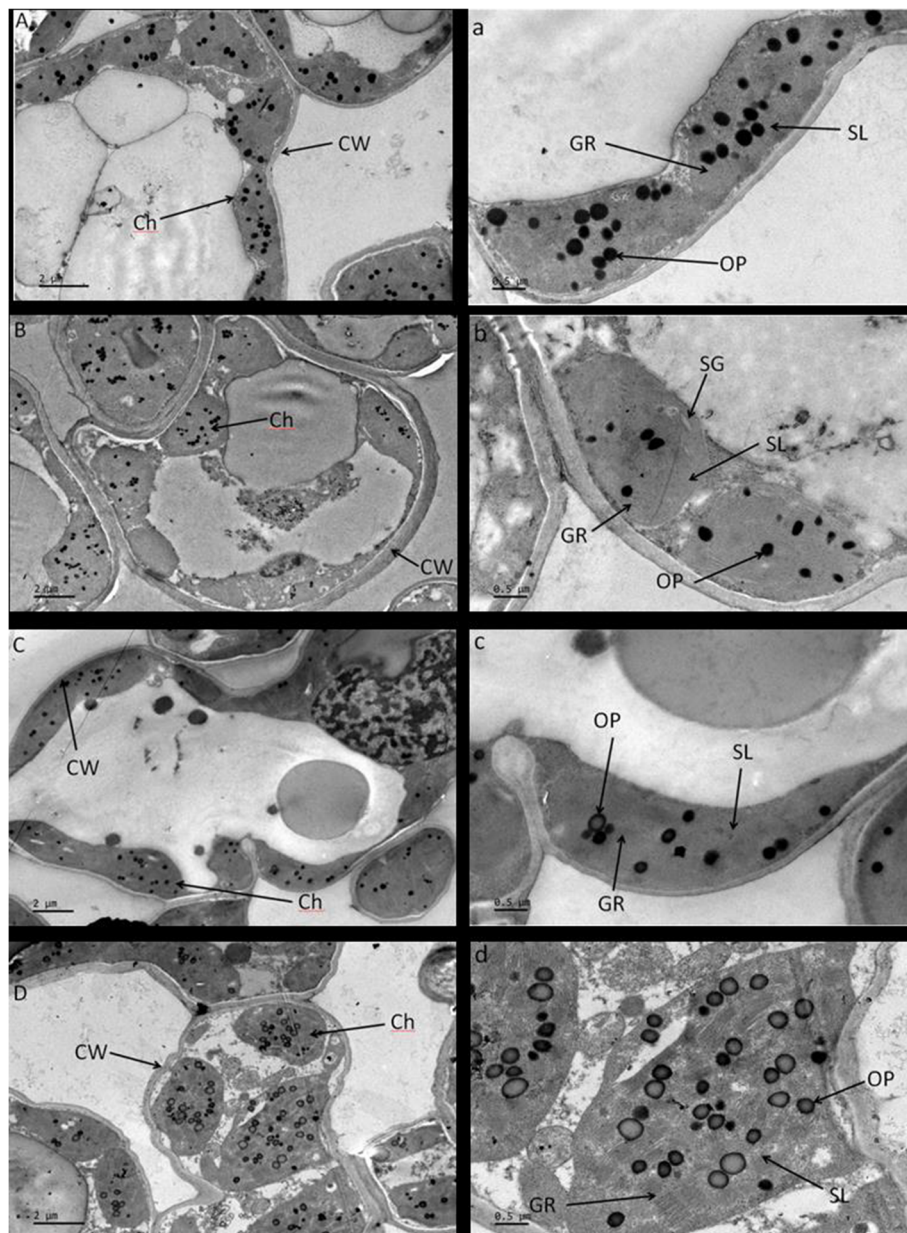
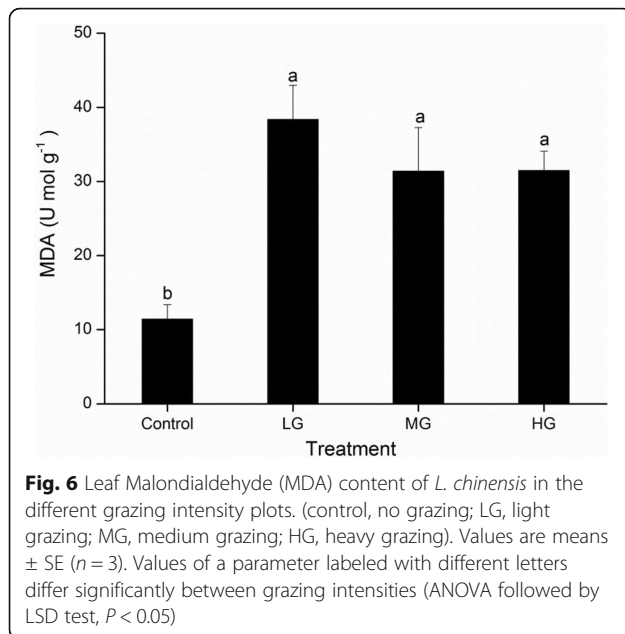


Fig. 5 The ultrastructure of the leaf cell of *L. chinensis* in the different grazing intensity plots (control, no grazing; LG, light grazing; MG, medium grazing; HG, heavy grazing). **a** control, **b** LG, **c** MG, **d** HG. Abbreviations: CW, cell wall; SL, stroma lamellae; G, granum; SG, starch grain; P, plastoglobuli. The scale bars for the whole cell (top row) and the enlarged parts (bottom row) are 2 and 0.5 μm , respectively

reduced in time and are therefore converted into starch, resulting in the accumulation of starch granules in the chloroplast.

The Chl *b* content did not differ significantly among the four plots, suggesting that this pigment was not sensitive to grazing stress. However, with increasing grazing intensity, the Chl *a* content increased, which suggests that the plants responded to the more serious grazing stress by increasing the amount of the photosystem components used to improve photosynthetic efficiency by improving

electron transfer among the reaction centers [21, 55]. In the MG and HG plots, the Car contents were higher than in the LG plot, which represents a protective mechanism for the photosystem. Car reacts with lipid peroxidation products and removes singlet oxygen [57]. The high Car content in the two most severely grazed plots would promote energy transfer from the chlorophyll molecules to a chlorophyll zeaxanthin heterodimer, thereby assisting with the dissipation of excess energy [32, 58]. Therefore, ROS accumulation decreased in the two plots, although the



decrease was not significant. Especially in the MG plots, more energy was used for thermal energy dissipation (62%) and less was used for photosynthetic electron transport (19%). The higher NPQ in these plots suggests that that photosynthetic apparatus dissipated the excessive energy as heat and protected against photoinhibition [59, 64]. Φ_{PSII} represents the quantum efficiency of photochemical reactions and is negatively correlated with NPQ [72]. Therefore, with lower Φ_{PSII} in the MG plots, the photosynthetic rate decreased compared to the other plots. This also explains why the C accumulation in the leaves was lower in these plots.

Our results suggest that compensatory photosynthesis occurred in the HG plots. More energy was used for the photosynthetic electron transport (27%) than in the other plots (19 to 25%), thereby increasing the photosynthetic rate compared with the other grazed plots. With increasing grazing intensity, the transpiration rate of leaves increases. Plants in the HG plots therefore increased their WUE compared to the other grazing plots to maintain growth. Furthermore, plants absorbed more nutrient elements from the soil, which affected the photosynthesis [1]. The leaf N contents were highest in the HG plots. The significantly increased $J_{\text{max}}/V_{\text{cmax}}$ ratio in the HG plots also suggested that the plants invested more N in Rubisco carboxylation [47]. The high N content, photosynthetic pigment, Rubisco activity, and more energy in the photosynthetic electron transport all indicated the compensatory photosynthesis of plants in the HG plots [19]. Though the chloroplasts were clearly damaged in the HG plots, adjustment of the plant's internal mechanisms improved the compensatory photosynthesis. A certain

degree of herbivore stimulated the increase of photosynthetic rate. In contrast, the increased leaf P contents in the LG plots suggest increased sensitivity of V_{cmax} to the leaf N content [79]. We hypothesize that there was a trade-off between the photosynthetic gains and energy dissipation costs to improve survival of the plants. In other hand, the adjustment of photosynthesis in the different intensity grazing plots was also influenced by the change of community. In general, the leaf area index (LAI) decreased significantly with the drop of above-ground biomass. That's one of the reasons the photosynthetic capacity decreased in the grazing plots. However, the relationship between the photosynthetic adjustment and community change in the different grazing plots still need to be further discussed with data support. Besides, the compensatory photosynthesis cannot be confined to the defoliation simply. The other environmental factors including the nutrients and water also should be taken into account [3].

ROS regulation under different grazing intensities

Under grazing, excess light will contribute to the production of ROS, which directly damage the cell and chloroplast membranes [38]. Under these circumstances, malondialdehyde is produced, so the malondialdehyde level provides a good proxy for oxidative damage [48, 52]. In this study, the MDA contents of the leaves in the grazing plots were significantly higher than those in the control plots, which suggest that grazing stress resulted in increased lipid peroxidation in the cell membrane. Furthermore, as the main organ affected by herbivores, leaves have higher MDA contents, thereby increasing the contents of free fatty acids and free sterols and decreasing the fluidity of the cell membrane [50]. Especially in the LG plots, lipid peroxidation was serious and would have led to photodamage of PSII in the chloroplasts [47]. As we noted earlier in the Discussion, the high Car content could quench the trilinear chlorophyll before it reacts with oxygen, and could also quench singlet oxygen [58]. Therefore, a high Car content could have helped to decrease the ROS content in the MG and HG plots.

Once the ROS content increases to a certain level, the antioxidant system will be activated to scavenge the ROS [4, 35, 38]. SOD is the first line of defense against ROS and will convert superoxide radicals into H_2O_2 [52]. Then peroxidase and catalase convert H_2O_2 into harmless H_2O and O_2 . In this study, the activity of superoxide dismutase was similarly high in the control, LG, and MG plots, but significantly lower in the HG plots, suggesting that the highest level of grazing stress suppressed the activity of this enzyme because the higher P_n used up more light energy and therefore reduced production of ROS compared to the other grazing levels. However, high activity of SOD alone may not have been

sufficient to increase tolerance of grazing stress and decrease membrane lipid peroxidation damage in the LG plots [2]. The MG plots had the highest catalase activity. In contrast, when the SOD and CAT activity decreased, POD activity increased significantly in the HG plots. The significant increase in both POD and CAT enzymes with increasing grazing intensity suggests that superoxide dismutase converted much of the ROS into H₂O₂, which these enzymes then converted into O₂.

The balance among the activity of different antioxidant enzymes is crucial for decreasing the ROS level [4, 11]. In addition, the increased water stress in the grazing plots (indicated by significant decreases in the leaf osmotic potential at the two highest grazing intensities) would have induced the generation of ROS. However, the production of these antioxidant enzymes was not adequate to mitigate the negative influence of the ROS. Therefore, the accumulation of proline in the MG plots would have increased the osmotic potential to protect the cell [38, 54]. In the present study, the low leaf osmotic potential in the MG plots would transmit a signal that would accelerate the production of proline. The proline increase in MG plots could compensate for this decrease of the antioxidant enzymes [33].

These results show how the grazed plants adapted a combination of various strategies to mitigate the effects of ROS generation or to scavenge excess ROS and counteract the grazing stress.

Conclusions

We found that under grazing disturbance, *L. chinensis* adopted a range of strategies to growth. When the grazing pressure was light to medium, *L. chinensis* exhibited decreased photosynthetic capacity. More light was absorbed, but the excess energy could not be dissipated sufficiently fast, leading to damage to the photosynthetic apparatus and accumulation of ROS, as indicated by the high level of MDA. The accumulation of ROS also induced increased POD and CAT activity to protect the cell. A new equilibrium would therefore develop. Though the photosynthetic capacity decreased, the plant's productivity was not significantly decreased by light grazing. As the grazing intensity increased, *L. chinensis* began to reduce the production of ROS by increased thermal energy dissipation. The more energy that was dissipated, the less energy was used to support photosynthetic electron transport. At the same time, the increased herbivore intensity induced further declines in productivity. Under the heaviest grazing pressure, plant productivity (aboveground biomass) decreased sharply. Plants therefore changed their strategy to increase survival through photosynthetic compensation.

Our results suggest that the photosynthetic mechanisms of *L. chinensis* were able to adjust so as to acclimate to different levels of grazing intensity. The adjustments of

the photosynthetic enzymes, pigments, chlorophyll fluorescence parameters, and contents of antioxidant enzymes all contributed to this acclimation. The degree of photoinhibition depended on the balance between the plant's photosynthetic protection mechanisms and the damage to PSII. However, the relationship between photosynthetic performance and total productivity was not always consistent. More research will therefore be necessary to clarify this relationship.

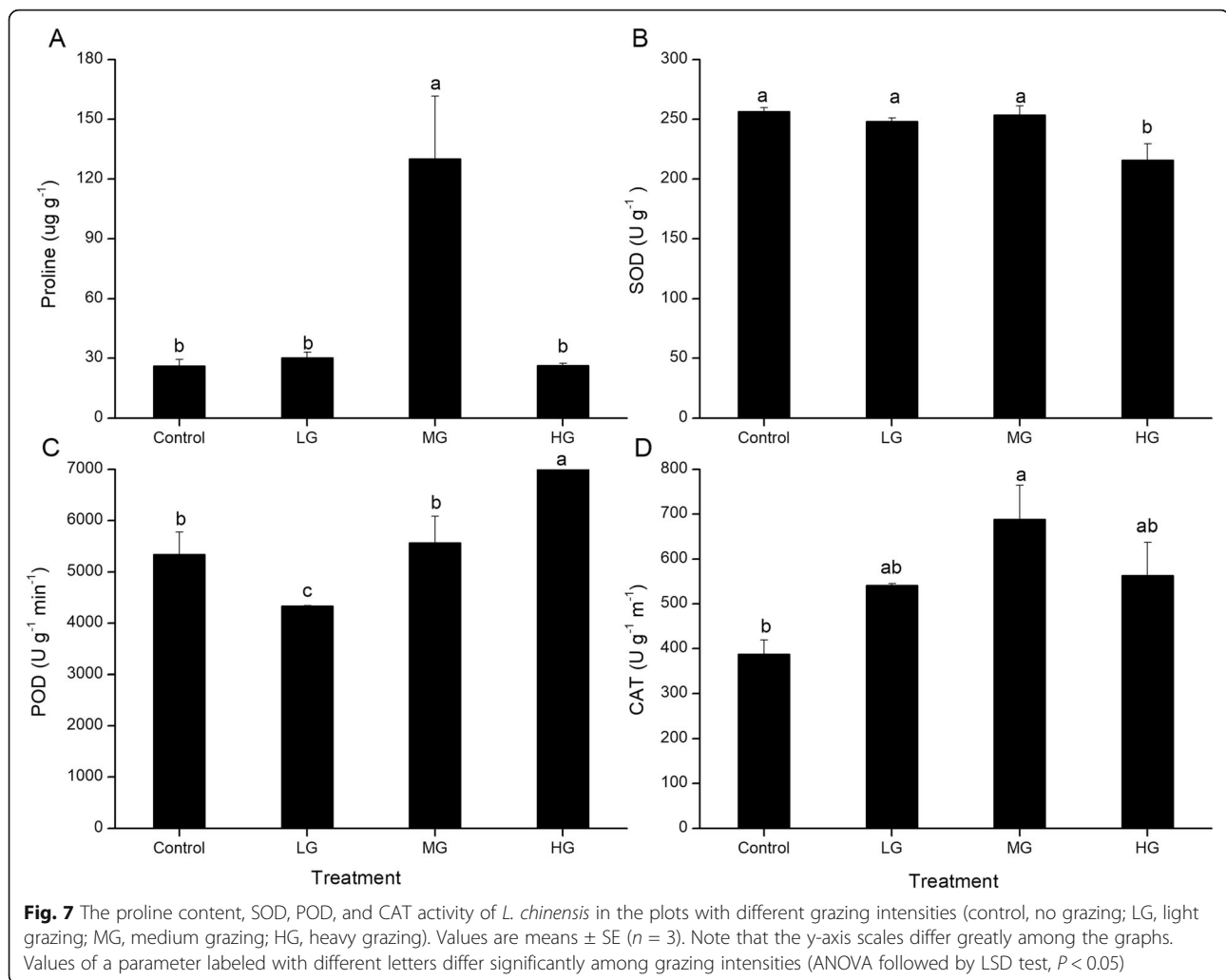
Methods

Study site and experimental design

The study was conducted at the Grassland Ecosystem Research Station of the Chinese Academy of Sciences (116°42'E, 43°38'N to 44°49'N) in Xilinhot, Inner Mongolia, China. This region has a typical temperate continental monsoon climate, with annual precipitation of 400 mm (of which 70% falls from June to August) and a mean annual temperature of 0.7 °C. The temperature ranges from a minimum of -41.1 °C in January to a maximum of 38.5 °C in August. The dominant species include *L. chinensis*, *Stipa grandis*, and *Stipa krylovii*. In June 2014, we began our grazing experiment, which lasted for 3 months. We designed four grazing intensity treatments: (1) a control, with no grazing; (2) light grazing (LG), with 4 sheep in each plot; (3) medium grazing (MG), with 8 sheep in each plot; and (4) heavy grazing (HG), with 12 sheep in each plot. Each plot was fenced to prevent changes in the number of sheep. Three replicates of each treatment were randomly assigned to 12 permanent plots, and each plot covered an area of 1.37 ha (Fig. 7). Each plot was about 125 m long and 110 m wide. The middle road was 5 cm wide. We chose *Leymus chinensis* (Trin.) TZvel., as the experimental subject in the 2016 growing season. We have permissions to collect such samples. The voucher specimen of *L. chinensis* was deposited in the Hulunbuir grassland ecosystem national field science research station of Inner Mongolia and the deposited number was 09-6045. The permission was obtained from the Grassland Ecosystem Research Station of the Chinese Academy of Sciences.

Plants morphological traits biomass, and soil traits

During mid-August 2016, we established three quadrats (1 m × 1 m) within each grazing plot. We then randomly selected 10 individuals of *L. chinensis* in each replicate to measure the plant height, tiller number, and internode length. The leaf fresh area, fresh mass, and oven-dry mass were measured to determine the specific leaf area (SLA), which equaled the fresh leaf area divided by the leaf oven-dry mass. We also measured the leaf osmotic potential using a model WP4C Dewpoint PotentialMeter (Decagon Devices, Pullman, WA, USA).



On the same date, we harvested the total above-ground biomass of *L. chinensis* to a height of 2 cm above the ground in the quadrats. The samples were then oven-dried at 65 °C to constant weight to determine the biomass. In addition, we ground the dried samples to a powder and then analyzed the powder to determine the leaf C, N, and P contents. The leaf C contents were determined by the Walkley-Black wet oxidation technique [56] with an automatic elemental analyzer (Vario EL, Elementar, Langensfeld, Germany). The leaf N contents were measured by the Kjeldahl method [9] with an automated Kjeldahl analyzer (Kjeltec 8400, Foss, Denmark). The leaf P contents were measured by inductively coupled plasma-atomic emission spectroscopy (ICP-AES) according to the method of Soon and Kalra [69]. In short, each sample and standard were weighted and mixed with nitric acid and H_2O_2 . Then they were placed in the Teflon tank and tightened by the stainless steel sleeve. Then the samples were heated at

160 °C for 4 h. After cooling, the samples were measured by the ICP-AES.

At the same time, we collected the 10–20 cm soil with plastic packaging bags. The soil C, N, and P contents were measured by the same methods. The fresh soil was weighed and then oven-dried at 105 °C to measure the dry mass. The soil water content was calculated by the following formulas:

$$\text{Soil water content} = (\text{fresh mass} - \text{dry mass}) / \text{fresh mass}$$

Leaf gas-exchange and chlorophyll fluorescence parameters

Leaf gas-exchange and chlorophyll fluorescence parameters were measured by a portable gas-exchange system (LI-6400; Li-Cor, Lincoln, NE, USA). We used the fluorescent chambers (LI-6400-40) with the red and blue light source, which including 90% red light and 10% blue light. For these measurements, we chose 10 individuals

of *L. chinensis* in each replicate of the four plots. For selecting plant samples, we chose the third leaf of each *L. chinensis* plant for photosynthetic measurements. The leaves were mature and healthy. We measured the instantaneous net photosynthetic rate (P_n) and transpiration rate (T_r), and then calculated the water-use efficiency (WUE) as P_n/T_r . We determined the light-response curves of *L. chinensis* at a CO_2 concentration of $380 \mu\text{mol mol}^{-1}$ and a photosynthetically active radiation ranging from 0 to $2500 \mu\text{mol m}^{-2} \text{s}^{-1}$. The photosynthetic photon flux density (PPFD) was set at 2500, 2000, 1500, 1000, 500, 200, 150, 100, 50, 20, and $0 \mu\text{mol m}^{-2} \text{s}^{-1}$. The light-saturation point (LSP), light-compensation point (LCP), dark respiration rate (R_d), and apparent quantum yield (AQY) were obtained from the light response curve. The calculation was based on the corrected nonrectangular hyperbolic model [74].

The CO_2 response curves were measured with the CO_2 concentration ranging from 0 to $1800 \mu\text{mol mol}^{-1}$. The CO_2 concentration was set at 400, 300, 200, 150, 100, 50, 400, 400, 600, 800, 1000, 1200, 1500, and $1800 \mu\text{mol mol}^{-1}$. We calculated the maximum electron transport rate (J_{max}), the maximum carboxylation efficiency (V_{cmax}), and the triose phosphate utilization rate (V_{TPU}) using the biochemical model of photosynthetic CO_2 assimilation [23].

The plants were measured in a randomized order between 09:00 and 11:00 am. To make the conditions as consistent as possible, we set the same leaf external environment. The flow rate was set as $500 \mu\text{mol s}^{-1}$ and the leaf temperature was 28°C .

Chlorophyll fluorescence parameters were also measured by the Li-Cor LI-6400. Before the measurements, leaves must be wrapped with tinfoil for dark adaptation at the ambient temperature. The dark adaptation lasted for at least 40 min. The maximum fluorescence (F_m) and minimum fluorescence (F_0) in the dark-adapted state were recorded simultaneously in the darkness. Next, the leaves were exposed to a PPFD of $1000 \mu\text{mol photons m}^{-2} \text{s}^{-1}$ for more than 10 min to measure the minimum fluorescence (F_0'), the maximum fluorescence (F_m'), and the steady-state fluorescence (F_s) in the light-adapted state after P_n stabilized. We then calculated the maximum quantum efficiency of photosystem II (PSII; F_v/F_m), the energy harvesting efficiency of PSII (F_v'/F_m'), the photochemical quenching coefficient (q_p), the non-photochemical quenching coefficient (NPQ), the electron transport rate (ETR), the effective quantum yield of PSII (Φ_{PSII}), and the energy partitioning among photosynthetic electron transport energy (P), the thermal energy dissipation (D), and excess energy (E) according to the methods of Demmig-Adams et al. [14].

$$P = (F'_m - F_s) / F'_m$$

$$D = 1 - (F'_v / F'_m)$$

$$E = (F'_v / F'_m) \times (1 - q_p)$$

Leaf photosynthetic pigments and Rubisco activity

After measuring of photosynthesis, we selected the plants and immediately collected the leaves. The fresh samples was weighted and packaged in 0.5 g by the brown paper. Then the samples were frozen in liquid nitrogen for subsequent biochemical analyses.

We extracted the chlorophyll a (Chl *a*), chlorophyll b (Chl *b*), and carotenoids (Car) from the leaves using 95% ethanol at 25°C in the darkness. We measured the absorbance of the resulting solutions at 470, 649, and 665 nm, respectively, using the 756PC ultraviolet-visible spectrophotometer. We then calculated the pigment contents using the equations of Fargašová [22].

We measured the Rubisco activity in the leaves according to the method of Wang et al. [80]. In short, the frozen samples were ground in extraction solution that contained 0.1 mol/L Tris-HCL, 12 mmol/L MgCl_2 , 0.36 mmol/L EDTA, and 5 mmol/L β -mercaptoethanol. We then centrifuged the solution at $1500g$ and 4°C for 15 min. We mixed 0.5 mL of the supernatant with 1 mol/L Tris-HCL (pH = 8.0), 2 mmol/L NADH, 0.1 mol/L MgCl_2 , 50 mmol/L DTT, 2 mol/L KHCO_3 , 1 mmol/L EDTA, and 160 U/L 3-phosphoglyceric phosphokinase. We then measured the absorbance at 340 nm using the 756PC ultraviolet-visible spectrophotometer to calculate the Rubisco activity.

$$\text{the Rubisco activity} = \frac{\Delta\text{OD}_{340} \times V_t}{2 \times T \times V_s \times W \times 6.22}$$

ΔOD_{340} was the change absorbance in the reaction time. Two means that 2 mol NADH was oxidized when 1 mol CO_2 was fixed. T was the reaction time. V_t was the extracting solution volume. V_s was the volume of the reaction solution. W was the weight of the sample. Six point twenty-two was the extinction coefficient of $1 \mu\text{mol NADH}$.

The lipid peroxidation and antioxidant systems and proline contents

We used the malondialdehyde (MDA) content as a proxy for the level of lipid peroxidation. We measured the MDA content according to the thiobarbituric acid reaction [16]. The samples (0.5 g) were ground in 5% trichloroacetic acid (TCA) solution and then centrifuged at $1500g$ for 10 min. The supernate was mixed with 0.67% thiobarbital acid (TBA) solution. The solution was boiled and centrifuged again. We measured the absorbance at 450 nm, 532 nm and 600 nm using the ultraviolet-visible spectrophotometer (756PC, Shanghai Jinghua, Shanghai, China). The MDA contents were calculated by the following formulas.

$$C_{MDA} = 6.45(OD_{532} - OD_{600}) - 0.56 OD_{450}$$

$$\text{The sample MDA content} = \frac{C_{MDA} \times V_t}{V_s \times W}$$

C_{MDA} was the concentration of MDA in the reaction solution. V_t was the extracting solution volume. V_s was the volume of the reaction solution. W was the weight of the sample.

We measured the activities of the antioxidant enzymes (SOD, POD and CAT) according to the methods of Gong et al. [24]. The sample (0.5 g) was ground in liquid nitrogen and extracted in the sodium phosphate buffer (pH 7.0). The extracting solution was centrifuged at 15000 g for 20 min at 4 °C. The resulting supernatant was used for the enzyme assays. One unit of the SOD activity was defined as the amount enzyme required to inhibit the reduction of nitroblue tetrazolium (NBT) by half. The reaction solution contained 50 mM sodium phosphate buffer (pH 7.8) with 100 μ M Na₂-EDTA, 130 mM methionine, 750 μ M NBT, 20 μ M riboflavin and 0.1 ml enzyme extract. Reactions were performed at 4000 lx irradiance by the fluorescent lamp for 20 min. Reaction in the dark was the blank control group. We measured the absorbance at 560 nm and calculated the enzyme activity.

$$\text{The SOD activity} = \frac{(OD_{CK} - OD) \times V_t}{OD_{CK} \times V_s \times W \times 0.5}$$

OD_{CK} and OD were the absorbance of the blank control and samples, respectively. V_t was the extracting solution volume. V_s was the volume of the reaction solution. W was the weight of the sample.

When measuring the POD activity, the enzyme extract was mixed with the reaction solution which included 100 mM potassium phosphate buffer (pH 7.0), 20 mM guaiacol, and 20 mm³ H₂O₂. The absorbance value at 470 nm was immediately determined and recorded every 30 s for 4 min. POD activity was calculated according to the change of absorbance according to the formula.

$$\text{The POD activity} = \frac{\Delta OD_{470} \times V_t}{T \times V_s \times W \times 0.01}$$

ΔOD_{470} was the change absorbance in the reaction time. T was the reaction time. V_t was the extracting solution volume. V_s was the volume of the reaction solution. W was the weight of the sample.

When measuring the CAT activity, the enzyme extract was mixed with 20 mM H₂O₂ and the sodium phosphate buffer (PH 7.0). Then we measured the decrease in absorbance at 240 nm every 30 s for 4 min.

$$\text{The CAT activity} = \frac{\Delta OD_{240} \times V_t}{T \times V_s \times W \times 0.1}$$

ΔOD_{240} was the change absorbance in the reaction time. T was the reaction time. V_t was the extracting

solution volume. V_s was the volume of the reaction solution. W was the weight of the sample.

We determined the proline content by the ninhydrin coloration method with some modification [8]. The samples (0.5 g) were ground in 5 ml 3% sulfosalicylic acid to boiling and centrifugation. Then 2 ml supernatant was mixed with 2 ml distilled water, 2 ml glacial acetic acid and 4 ml ninhydrin and boiled at 100 °C for 60 min. After cooling, we added toluene and measured the absorbance at 520 nm. The standard curve of proline was obtained by the same way.

$$\text{The sample proline content} = \frac{C \times V_t}{V_s \times W}$$

C was the content of proline from the standard curve. V_t was the extracting solution volume. V_s was the volume of the reaction solution. W was the weight of the sample.

Ultrastructure of the leaf cells

We examined the ultrastructure of the leaf cells by means of transmission electron microscopy [39]. We collected fresh leaves from the four plots (control, LG, MG, HG), then cut them into small pieces (1 mm × 1 mm × 2 mm) and fixed them in 4% glutaraldehyde solution at 4 °C. After washing the samples five times with 0.1 mol/L phosphate buffer, the materials were fixed overnight in 1% osmic acid at 4 °C. The materials were then dehydrated using an acetone series of 30, 50, 70, 85, 95, and 100% v/v (for 10 min at each concentration, 2 times). The materials were then infiltrated with acetone and resin: at proportions of 3:1 v/v, 1:1 v/v, and 1:2 v/v, in that order, with each infiltration conducted for 3 h the proportion was 3:1; 1:1; 1:2 respectively for 3 h followed by infiltration with 100% resin for 12 h. After polymerization at 60 °C for 24 h, we created thin-sections using an ultramicrotome (Leica Microsystems, Bensheim, Germany) and double-stained the sections with uranyl acetate–lead citrate. We examined the samples using a model JEM1230 transmission electron microscope (JEOL, Tokyo, Japan).

Data and statistical analysis

Statistical tests were carried out using version 20.0 of SPSS (SPSS Inc., Chicago, IL, USA). We tested for significant differences among the four grazing intensities using one-way analysis of variance (ANOVA), with significance at $P < 0.05$. When the ANOVA result was significant, we used least-significant-difference (LSD) tests to identify differences in the morphological and physiological traits between pairs of treatments. Before using ANOVA, normality of the data was tested by Kolmogorov-Smirnov

Test. All graphs were created using version 8.5 of the Origin software (<https://www.originlab.com/>).

Abbreviations

AQY: Apparent quantum yield; CAT: Catalase; Ch: Chlorophyll; CW: Cell wall; D: Thermal dissipation; D : Thermal energy dissipation; E : Excess energy; ETR: Electron transport rate; F_m : Maximum fluorescence yield in the dark-adapted state; F_m' : Maximum fluorescence yield in the light-adapted state; F_o : Minimum fluorescence yield in the dark-adapted state; F_o' : Minimum fluorescence yield in the light-adapted state; F_s : Steady-state fluorescence; F_v' : Variable fluorescence in the light-adapted state; GR: Granum; HG: Heavy grazing; J_{max} : The maximum electron transport rate; LCP: Light-compensation point; LG: Light grazing; LSP: Light-saturation point; MDA: Malondialdehyde; MG: Medium grazing; NBT: Nitroblue tetrazolium; NPQ: Non-photochemical quenching coefficient; OP: Osmiophilic granule; P : Photosynthetic electron transport energy; P_n : Net photosynthetic rate; POD: Peroxidase; $PPFD$: Photosynthetic photon flux density; q_p : Photochemical quenching coefficient; R_d : Dark respiration rate; ROS: Reactive oxygen species; Rubisco: Ribulose 1,5-bisphosphate carboxylase; SL: Stroma lamellae; SOD: Superoxide dismutase; TBA: Thiobarbital acid; TCA: Trichloroacetic acid; T_r : Transpiration rate; V_{cmax} : The maximum carboxylation efficiency; V_{TPU} : The triose phosphate utilization rate; WUE: Water-use efficiency; Φ_{PSII} : Effective quantum yield of PSII

Acknowledgements

Not Applicable

Authors' contributions

JG and XH planned and designed the research. XH and YD provided guidance in the field experiments. ML, BY, ZZ, BW, CZ and YD performed most of the fieldwork. ML conducted most of the laboratory experiments. JG and ML analyzed data and wrote the manuscript. All authors have read and approved the manuscript, and ensure that this is the case.

Funding

This study was supported by the National Natural Science Foundation of China (Grant No. 41571048), the Key National R & D program of China (Grant No. 2016YFC0500502), and the State Key Basic Research and Development Plan of China (Grant No. 2014CB138803).

Availability of data and materials

The datasets generated and/or analysed during the current study are not publicly available but are available from the corresponding author on reasonable request.

Ethics approval and consent to participate

Not Applicable

Consent for publication

Not Applicable.

Competing interests

The authors declare that they have no competing interests.

Author details

¹Beijing Key Laboratory of Traditional Chinese Medicine Protection and Utilization, Key Laboratory of Surface Processes and Resource Ecology, College of Resources Science and Technology, Faculty of Geographical Science, Beijing Normal University, No. 19 Xijiekouwai Street, Beijing 100875, China. ²Key Laboratory of Tourism and Resources, Environment in Taishan University, Taian 271021, China. ³Grassland Research Institute of Chinese Academic of Agricultural Science, Hohhot 010021, Inner Mongolia, China.

Received: 19 June 2019 Accepted: 3 December 2019

Published online: 16 December 2019

References

1. Ai ZM, Zhang JY, Liu HF, Xin Q, Xue S, Liu GB. Soil nutrients influence the photosynthesis and biomass in invasive *Panicum virgatum* on the loess plateau in China. *Plant Soil*. 2017;418:153–64.
2. Almeselmani M, Deshmukh PS, Sairam RK, Kushwaha SR, Singh TP. Protective role of antioxidant enzymes under high temperature stress. *Plant Sci*. 2006;171(3):382–8.
3. Anten NPR, Ackerly DD. Canopy-level photosynthetic compensation after defoliation in a tropical understorey palm. *Funct Ecol*. 2001;15(2):252–62.
4. Apel K, Hirt H. Reactive oxygen species: metabolism, oxidative stress, and signal transduction. *Annu Rev Plant Biol*. 2004;55:373–99.
5. Ashraf M, Harris PJC. Photosynthesis under stressful environments: an overview. *Photosynthetica*. 2013;51(2):163–90.
6. Barger NN, Ojima DS, Belnap J, Wang SP, Wang YF, Chen ZZ. Changes in plant functional groups, litter quality, and soil carbon and nitrogen mineralization with sheep grazing in an inner Mongolian grassland. *J Range Manag*. 2004;57(6):613–9.
7. Bateman A, Lewandrowski W, Stevens JC, Munoz-Rojas M. Ecophysiological indicators to assess drought responses of arid zone native seedlings in reconstructed soils. *Land Degrad Dev*. 2018;29:984–93.
8. Bates LS, Waldren RP, Teare ID. Rapid determination of free proline for water stress studies. *Plant Soil*. 1973;39:205–7.
9. Bremner JM. Determination of nitrogen in soil by the Kjeldahl method. *J Agric Sci*. 1960;55:11–33.
10. Chen C, Dickman MB. Proline suppresses apoptosis in the fungal pathogen *Colletotrichum trifolii*. *Proc Natl Acad Sci U S A*. 2005;102(9):3459–64.
11. Chen YH, Hung YC, Chen MY, Lin MS, Lin HT. Enhanced storability of blueberries by acidic electrolyzed oxidizing water application may be mediated by regulating ROS metabolism. *Food Chem*. 2019;270:229–35.
12. Chludil HD, Leicach SR, Corbino GB, Barriga LG, Vilariño MP. Genistin and quinolizidine alkaloid induction in *L. angustifolius* aerial parts in response to mechanical damage. *J Plant Interact*. 2013;8:117–24.
13. Crawford TS, Hanning KR, Chua JP, Eatonrye JJ, Summerfield TC. Comparison of D1⁻ and D1-containing PSII reaction Centre complexes under different environmental conditions in *Synechocystis* sp. PCC 6803. *Plant Cell Environ*. 2016;39(8):1715–26.
14. Demmig-Adams B, Adams WW, Barker DH, Logan BA, Bowling DR, Hoveen AS. Using chlorophyll fluorescence to assess the fraction of absorbed light allocated to thermal dissipation of excess excitation. *Physiol Plant*. 1996;98:253–64.
15. Detling JK, Dyer MI, Winn DT. Net photosynthesis, root respiration, and regrowth of *Bouteloua gracilis* following simulated grazing. *Oecologia*. 1979;41(2):127–34.
16. Dhindsa RS, Matowe W. Drought tolerance in two mosses: correlated with enzymatic defence against lipid peroxidation. *J Exp Bot*. 1981;32:79–91.
17. Díaz-Barradas MC, Zunzunegui M, Alvarez-Cansino L, Esquivias MP, Valera J, Rodríguez H. How do Mediterranean shrub species cope with shade? Ecophysiological response to different light intensities. *Plant Biol*. 2017;20(2):296–306.
18. Dinç E, Ceppi MG, Tóth SZ, Sandor B, Schansker G. The chl *a* fluorescence intensity is remarkably insensitive to changes in the chlorophyll content of the leaf as long as the chl *a/b* ratio remains unaffected. *Biochim Biophys Acta*. 2012;1817(5):770–9.
19. Doescher PS, Svejcar TJ, Jandl RG. Gas exchange of Idaho fescue in response to defoliation and grazing history. *J Range Manag*. 1997;50(3):285–9.
20. Dubreuil C, Jin X, de Dios B-LJ, Hewitt TC, Tanz SK, Dobrenel T, Schroder WP, Hanson J, Pesquet E, Gronlund A. Establishment of photosynthesis through chloroplast development is controlled by two distinct regulatory phases. *Plant Physiol*. 2018;176:1199–214.
21. Esteban R, Barrutia O, Artetxe U, Fernandez-Marin B, Hernandez A, Garcia-Plazaola JL. Internal and external factors affecting photosynthetic pigment composition in plants: a meta-analytical approach. *New Phytol*. 2015;206(1):268–80.
22. Fargašová A. Inhibitive effect of organotin compounds on the chlorophyll content of the green freshwater alga *Scenedesmus quadricauda*. *Bull Environ Contam Toxicol*. 1996;57(1):99–106.
23. Farquhar GD, Caemmerer SV, Berry JA. A biochemical model of photosynthetic CO₂ assimilation in leaves of C₃ species. *Planta*. 1980;149(1):78–90.
24. Gong JR, Zhao AF, Huang YM, Zhang XS, Zhang CL. Water relations, gas exchange, photochemical efficiency, and peroxidative stress of four plant species in the Heihe drainage basin of northern China. *Photosynthetica*. 2006;44(3):355–64.
25. Grime JP. Benefits of plant diversity to ecosystems: immediate, filter and founder effects. *J Ecol*. 1998;86:902–10.

26. Halitschke R, Hamilton JG, Kessler A. Herbivore-specific elicitation of photosynthesis by mirid bug salivary secretions in the wild tobacco *Nicotiana attenuata*. *New Phytol.* 2011;191(2):528–35.
27. Hamann PA, Czaja S, Hunsche M, Noga G, Fiebig A. Monitoring physiological and biochemical responses of two apple cultivars to water supply regimes with non-destructive fluorescence sensors. *Sci Hortic.* 2018;242(19):51–61.
28. Hanelt D, Huppertz K, Nultsch W. Photoinhibition of photosynthesis and its recovery in red algae. *Plant Biol.* 2015;105(4):278–84.
29. Harrison MT, Kelman WM, Moore AD, Evans JR. Grazing winter wheat relieves plant water stress and transiently enhances photosynthesis. *Funct Plant Biol.* 2010;37(8):726–36.
30. Hayashi M, Fujita N, Yamauchi A. Theory of grazing optimization in which herbivory improves photosynthetic ability. *J Theor Biol.* 2007;248(2):367–76.
31. Hazrati S, Tahmasebi-Sarvestani Z, Modarres-Sanavy SAM, Mokhtassi-Bidgoli A, Nicolab S. Effects of water stress and light intensity on chlorophyll fluorescence parameters and pigments of *Aloe vera* L. *Plant Physiol Biochem.* 2016;106:141–8.
32. Holt NE, Zigmantas D, Valkunas L, Li XP, Niyogi KK, Fleming GR. Carotenoid cation formation and the regulation of photosynthetic light harvesting. *Science.* 2005;307(5708):433–6.
33. Hoque MA, Okuma E, Banu MNA, Nakamura Y, Shimoishi Y, Murata Y. Exogenous proline mitigates the detrimental effects of salt stress more than exogenous betaine by increasing antioxidant enzyme activities. *J Plant Physiol.* 2007;164(5):553–61.
34. Huang J, Zhang PJ, Zhang J, Lu YB, Huang F, Li MJ. Chlorophyll content and chlorophyll fluorescence in tomato leaves infested with an invasive mealybug, *Phenacoccus solenopsis* (Hemiptera: Pseudococcidae). *Environ Entomol.* 2013;42(5):973–9.
35. Jiang XJ, Lin HT, Lin MS, Chen YH, Wang H, Lin YX, Shi J, Lin YF. A novel chitosan formulation treatment induces disease resistance of harvested litchi fruit to *Peronophythora litchii* in association with ROS metabolism. *Food Chem.* 2018;66:299–308.
36. Jimenez-Rodríguez DL, Alvarez-Añorbe MY, Pineda-Cortés M, Flores-Puerto JI, Benitez-Malvido J, Oyama K, Avila-Cabadilla LD. Structural and functional traits predict short term response of tropical dry forests to a high intensity hurricane. *For Ecol Manag.* 2018;426:101–14.
37. Kang L, Han XG, Zhang ZB, Sun OJ. Grassland ecosystems in China: review of current knowledge and research advancement. *Philos Trans R Soc Lond Ser B Biol Sci.* 2007;362:997–1008.
38. Kurepin LV, Ivanov AG, Zaman M, Pharis RP, Allakhverdiev SI, Hurry V, Huner NPA. Stress-related hormones and glycinebetaine interplay in protection of photosynthesis under abiotic stress conditions. *Photosynth Res.* 2015;126(2–3):221–35.
39. Li LY, Yang HM, Ren WB, Liu B, Cheng DM, Wu XH, Gong JR, Peng LW, Huang F. Physiological and biochemical characterization of sheepgrass (*Leymus chinensis*) reveals insights into photosynthetic apparatus coping with low-phosphate stress conditions. *J Plant Biol.* 2016a;59:336–46.
40. Li XJ, Guo X, Zhou YH, Shi K, Zhou J, Yu JQ, Xia XJ. Overexpression of a brassinosteroid biosynthetic gene dwarf enhances photosynthetic capacity through activation of Calvin cycle enzymes in tomato. *BMC Plant Biol.* 2016b;16(1):1–12.
41. Liu CX, Zou DH, Yang YF, Chen BB, Jiang H. Temperature responses of pigment contents, chlorophyll fluorescence characteristics, and antioxidant defenses in *Gracilaria lemaneiformis* (Gracilariiales, Rhodophyta) under different CO₂ levels. *J Appl Phycol.* 2017b;29(2):983–91.
42. Liu M, Gong JR, Pan Y, Luo QP, Zhai ZW, Xu S, Yang LL. Effects of grass-legume mixtures on the production and photosynthetic capacity of constructed grasslands in Inner Mongolia, China. *Crop Pasture Sci.* 2016;67:1188–98.
43. Liu SL, Tang YH, Zhang FW, Du WG, Lin L, Li YK, Guo XW, Li Q, Cao GM. Changes of soil organic and inorganic carbon in relation to grassland degradation in northern Tibet. *Ecol Res.* 2017a;32(3):1–10.
44. Liu TF, Zhang CL, Yang GS, Wu JS, Xie GS, Zeng HL, Yin CX, Liu TM. Central composite design-based analysis of specific leaf area and related agronomic factors in cultivars of rapeseed (*Brassica napus* L.). *Field Crop Res.* 2009; 111(1):92–6.
45. Liu YS, Yang XH, Tian DS, Cong RC, Zhang X, Pan QM, Shi ZJ. Resource reallocation of two grass species during regrowth after defoliation. *Front Plant Sci.* 2018;9:1–11.
46. Lu T, Meng ZJ, Zhang GX, Qi MF, Sun ZP, Liu YF, Li TL. Sub-high temperature and high light intensity induced irreversible inhibition on photosynthesis system of tomato plant (*Solanum lycopersicum* L.). *Front Plant Sci.* 2017a;8:1–16.
47. Lu ZF, Pan YH, Hu WS, Cong RH, Ren T, Guo SW. The photosynthetic and structural differences between leaves and siliques of *Brassica napus* exposed to potassium deficiency. *BMC Plant Biol.* 2017b;17(1):1–14.
48. Ma J, Lv CF, Xu ML, Chen GX, Lv CG, Gao ZP. Photosynthesis performance, antioxidant enzymes, and ultrastructural analyses of rice seedlings under chromium stress. *Environ Sci Pollut Res Int.* 2016;23(2):1768–78.
49. Machado RAR, Baldwin IT, Matthias E. Herbivory-induced jasmonates constrain plant sugar accumulation and growth by antagonizing gibberellin signaling and not by promoting secondary metabolite production. *New Phytol.* 2017;215:803–12.
50. Mansour MMF, Salama KHA, Ali FZM, Abou Hadid AF. Cell and plant responses to NaCl in *Zea mays* L. cultivars differing in salt tolerance. *Gen Appl Plant Physiol.* 2005;31(1–2):29–41.
51. Maxwell K, Johnson GN. Chlorophyll fluorescence—a practical guide. *J Exp Bot.* 2000;51(345):659–68.
52. Merchán FL, Merino P. Effect of salt stress on antioxidant enzymes and lipid peroxidation in leaves in two contrasting corn, ‘Llutenó’ and ‘Jubilee’. *Chil J Agric Res.* 2014;74(1):89–95.
53. Mlinarić S, Antunović DJ, Skendrović BM, Cesar V, Hrvoje L. Differential accumulation of photosynthetic proteins regulates diurnal photochemical adjustments of PSII in common fig (*Ficus carica* L.) leaves. *J Plant Physiol.* 2017;209:1–10.
54. Mohammadi H, Ghorbanpour M, Brestic M. Exogenous putrescine changes redox regulations and essential oil constituents in field-grown *Thymus vulgaris* L. under well-watered and drought stress conditions. *Ind Crop Prod.* 2017;209:1–10.
55. Neilsen JAD, Rangrikphoti P, Durnford DG. Evolution and regulation of *Bigeloviella natans* light-harvesting antenna system. *J Plant Physiol.* 2017; 217:68–76.
56. Nelson DW, Sommers LE. Total carbon, organic carbon and organic matter. In: Page AL, Miller RH, Keeney DR, editors. *Methods of soil analysis*. Madison: American Society of Agronomy; 1996. p. 961–1010.
57. Paliwal C, Pancha I, Ghosh T, Maurya R, Chokshi K, Bharadwaj SW, Ram S, Mishra S. Selective carotenoid accumulation by varying nutrient media and salinity in *Synechocystis* sp. CCNM 2501. *Bioresour Technol.* 2015;197:363–8.
58. Park S, Fischer AL, Steen CJ, Masakazu I, Morris JM, Walla PJ, Niyogi KK, Fleming GR. Fleming chlorophyll-carotenoid excitation energy transfer in high-light-exposed thylakoid membranes investigated by snapshot transient absorption spectroscopy. *J Am Chem Soc.* 2018;140(38):11965–73.
59. Pinnola A, Dall’Osto L, Gerotto C, Morosinotto T, Bassi R, Alboresi A. Zeaxanthin binds to light-harvesting complex stress-related protein to enhance nonphotochemical quenching in *Physcomitrella patens*. *Plant Cell.* 2013;25(9):3519–34.
60. Poorter H, Niinemets U, Walter A, Fiorani F, Schurr U. A method to construct dose–response curves for a wide range of environmental factors and plant traits by means of a meta-analysis of phenotypic data. *J Exp Bot.* 2010;61(8): 2043–55.
61. Qian L, Qi SZ, Cao FJ, Zhang J, Zhao F, Li CP, Wang CJ. Toxic effects of boscalid on the growth, photosynthesis, antioxidant system and metabolism of *Chlorella vulgaris*. *Environ Pollut.* 2018;242:171–81.
62. Ren WB, Hu NN, Hou XY, Zhang JZ, Guo HQ, Liu ZY, Kong LQ, Wu ZN, Wang H, Li XL. Long-term overgrazing-induced memory decreases photosynthesis of clonal offspring in a perennial grassland plant. *Front Plant Sci.* 2017;8:1–13.
63. Rivas R, Frosi G, Ramos DG, Pereira S, Benko-Iseppon AM, Santos MG. Photosynthetic limitation and mechanisms of photoprotection under drought and recovery of *Calotropis procera*, an evergreen C₃ from arid regions. *Plant Physiol Biochem.* 2017;118:589–99.
64. Ruban AV. Non-photochemical chlorophyll fluorescence quenching: mechanism and effectiveness in protection against photodamage. *Plant Physiol.* 2016;170(4):1903–16.
65. Ruiz-R N, Ward D, Saltz D. Leaf compensatory growth as a tolerance strategy to resist herbivory in *Pancratium sickenbergeri*. *Plant Ecol.* 2007; 198(1):19–26.
66. Salvucci ME, Crafts-Brandner SJ. Inhibition of photosynthesis by heat stress: the activation state of Rubisco as a limiting factor in photosynthesis. *Physiol Plant.* 2004;120(2):179–86.

67. Schönbach P, Wan HW, Gierus M, Bai YF, Müller K, Lin LJ, et al. Grassland responses to grazing: effects of grazing intensity and management system in an inner Mongolian steppe ecosystem. *Plant Soil*. 2011;340(1–2):103–15. <https://doi.org/10.1007/s11104-010-0366-6>.
68. Shen HH, Wang SP, Tang YH. Grazing alters warming effects on leaf photosynthesis and respiration in *Gentiana straminea*, an alpine forb species. *J Plant Ecol*. 2013;6(5):418–27.
69. Soon YK, Kalra YP. A comparison of plant tissue digestion methods for nitrogen and phosphorus analyses. *Can J Soil Sci*. 1995;75:243–5.
70. Stagnari F, Mattia CD, Galieni A, Santarelli V, D'Egidio S, Pagnani G, Pisante M. Light quantity and quality supplies sharply affect growth, morphological, physiological and quality traits of basil. *Ind Crop Prod*. 2018;122:277–89.
71. Takagi D, Takumi S, Hashiguchi M, Sejima T, Miyake C. Superoxide and singlet oxygen produced within the thylakoid membranes both cause photosystem I photoinhibition. *Plant Physiol*. 2016;171(3):1626–34.
72. Tang S, Zhang HX, Li L, Liu X, Chen L, Chen WZ, Ding YF. Exogenous spermidine enhances the photosynthetic and antioxidant capacity of rice under heat stress during early grain-filling period. *Funct Plant Biol*. 2018;45(9):911–21.
73. Terashima I, Sakaguchi S, Hara N. Intra-leaf and intracellular gradients in chloroplast ultrastructure of dorsiventral leaves illuminated from the adaxial or abaxial side during their development. *Plant Cell Physiol*. 1986;27:1023–31.
74. Thornley JHM. *Mathematical models in plant physiology*. London: Academic Press; 1976. p. 86–110.
75. Tikkanen M, Mekala NR, Aro EM. Photosystem II photoinhibition-repair cycle protects photosystem I from irreversible damage. *Biochim Biophys Acta*. 2014;1837(1):210–5.
76. van Staalduinen MA, Anten NPR. Differences in the compensatory growth of two co-occurring grass species in relation to water availability. *Oecologia*. 2005;146:190–9.
77. Vesik PA, Leishman MR, Westoby M. Simple traits do not predict grazing response in Australian dry shrublands and woodlands. *J Appl Ecol*. 2004;41:22–31.
78. Villar R, Ruiz-Robledo J, Uberta JL, Poorter H. Exploring variation in leaf mass per area (LMA) from leaf to cell: an anatomical analysis of 26 woody species. *Am J Bot*. 2013;100(10):1969–80.
79. Walker AP, Beckerman AP, Gu L, Kattge J, Cernusak LA, Domingues TF, Scales JC, Wohlfahrt G, Wullschlegel SD, Woodward FI. The relationship of leaf photosynthetic traits— V_{cmax} and J_{max} —to leaf nitrogen, leaf phosphorus, and specific leaf area: a meta-analysis and modeling study. *Ecol Evol*. 2014;4(16):3218–35.
80. Wang GD, Kong FY, Zhang S, Meng X, Wang H, Meng QW. A tomato chloroplast-targeted DnaJ protein protects Rubisco activity under heat stress. *J Exp Bot*. 2015;66(11):3027–40.
81. Wang RZ. Photosynthetic pathway types of forage species along grazing gradient from the Songnen grassland, northeastern China. *Photosynthetica*. 2002;40(1):57–61.
82. Wu GL, Liu ZH, Zhang L, Hu TM, Chen JM. Effects of artificial grassland establishment on soil nutrients and carbon properties in a black-soil-type degraded grassland. *Plant Soil*. 2010;333(1):469–79.
83. Yan L, Zhou G, Zhang F. Effects of different grazing intensities on grassland production in China: a meta-analysis. *PLoS One*. 2013;8(12):e81466.
84. Yu KL, Pypker TG, Keim RF, Chen N, Yang YB, Guo SQ, Li WJ, Wang G. Canopy rainfall storage capacity as affected by sub-alpine grassland degradation in the Qinghai-Tibetan plateau, China. *Hydrol Process*. 2012;26(20):3114–23.
85. Zandalinas SI, Mittler R, Balfagón D, Arbona V, Gómez-Cadenas A. Plant adaptations to the combination of drought and high temperatures. *Physiol Plant*. 2018;162:2–12.
86. Zhang B, Thomas BW, Beck R, Liu K, Zhao ML, Hao XY. Labile soil organic matter in response to long-term cattle grazing on sloped rough fescue grassland in the foothills of the Rocky Mountains, Alberta. *Geoderma*. 2018;318:9–15.
87. Zhao W, Chen SP, Lin GH. Compensatory growth responses to clipping defoliation in *Leymus chinensis* (Poaceae) under nutrient addition and water deficiency conditions. *Plant Ecol*. 2008;196:85–99.
88. Zheng SX, Lan ZC, Li WH, Shao RX, Shan YM, Wan HW, Taube F, Bai YF. Differential responses of plant functional trait to grazing between two contrasting dominant C_3 and C_4 species in a typical steppe of Inner Mongolia, China. *Plant Soil*. 2011;340:141–55.
89. Zhou XT, Zhao HL, Cao K, Hu LP, Du TH, Baluška F, Zou ZR. Beneficial roles of melatonin on redox regulation of photosynthetic electron transport and synthesis of D1 protein in tomato seedlings under salt stress. *Front Plant Sci*. 2016;7:1–10.

Publisher's Note

Springer Nature remains neutral with regard to jurisdictional claims in published maps and institutional affiliations.

Ready to submit your research? Choose BMC and benefit from:

- fast, convenient online submission
- thorough peer review by experienced researchers in your field
- rapid publication on acceptance
- support for research data, including large and complex data types
- gold Open Access which fosters wider collaboration and increased citations
- maximum visibility for your research: over 100M website views per year

At BMC, research is always in progress.

Learn more biomedcentral.com/submissions

